

# Electron-Phonon Interaction in Aluminum SINIS

S. A. Lemzyakov, M. A. Tarasov<sup>ID</sup>, and V. S. Edelman

**Abstract**—A detailed analysis of power flow in superconductor-insulator-normal metal-insulator-superconductor (SINIS) structures with aluminum superconducting electrodes and normal metal absorber made of aluminum with suppressed superconductivity is carried out. From a comparison with the experimental results of measuring the current-voltage characteristics at temperatures from 0.087 K to 0.3 K, it was concluded that the power of the electron-phonon interaction is proportional to the difference of sixth powers of the electron and phonon temperatures. The previously applied relation with the difference of fifth powers leads to an almost twofold error in determining the power of the electron-phonon interaction and an estimate of the electron temperature that is underestimated by about 40 mK.

**Index Terms**—Superconducting devices, phonons.

## I. INTRODUCTION

WHEN used in low-temperature radiation receivers with tunneling structures superconductor-insulator-normal metal-insulator-superconductor (SINIS), the absorbed power can be estimated from the change in the temperature  $T_e$  of the electrons of the normal metal absorber [1], [2]. Under stationary conditions and the assumption that a Fermi distribution is established in the system of electrons, the absorbed power can be calculated using the formula for the electron - phonon interaction. In the classic work [3], as well as in [2] and in our earlier paper [4] the following expression was used

$$P_5 = P_{e-ph} = \Sigma v (T_e^5 - T_{ph}^5). \quad (1)$$

In which  $\Sigma$  – specific constant of interaction,  $v$  – volume of the normal metal absorber,  $T_e$  electron temperature,  $T_{ph}$  – phonon temperature. For the studied structures made of aluminum superconducting electrodes and normal electrode of aluminum with a thin underlayer of iron for suppression of superconductivity it was taken the value of  $\Sigma = 1.3 \cdot 10^9 \text{ W/m}^3 \text{ K}^5$  [2]. Due to the

Manuscript received September 16, 2021; revised December 8, 2021; accepted December 24, 2021. Date of publication December 29, 2021; date of current version January 21, 2022. This work was supported in part by a grant from the Russian Science Foundation (under Project 21-42-04421 “Tunable Josephson Metamaterials for Quantum Devices”), in part by The equipment of USU “Cryointegral” was used to carry out the research; USU is supported by a grant from the Ministry of Science and Higher Education of the Russian Federation, under Agreement 075-15-2021-667. (Corresponding author: Mikhail Tarasov.)

S. A. Lemzyakov was with the P. Kapitza Institute for Physical Problems RAS, Moscow, Russia. He is now with the Department of Applied Physics, Aalto University, 00076 Aalto, Finland (e-mail: lemserj@gmail.com).

M. A. Tarasov is with the V. Kotelnikov Institute of Radio Engineering and Electronics RAS, 125009 Moscow, Russia (e-mail: tarasov@hitech.cplire.ru).

V. S. Edelman is with the P. Kapitza Institute for Physical Problems RAS, 119334 Moscow, Russia (e-mail: vsedelman@yandex.ru).

Color versions of one or more figures in this article are available at <https://doi.org/10.1109/TASC.2021.3139261>.

Digital Object Identifier 10.1109/TASC.2021.3139261

Kapitza resistance at the metal – silicon substrate interface,  $T_{ph}$  is slightly higher than the temperature  $T_{base}$  of the substrate in thermal contact with the thermostat at a temperature  $T$ . In real experimental conditions, this difference, leading to a correction in the calculation of  $P_{e-ph}$  by 1-2%, can be neglected.

However, in [5], when analyzing electron cooling in SINIS structures, also manufactured using the aluminum technology, a different temperature dependence was adopted:

$$P_6 = P_{e-ph} = \Sigma v (T_e^6 - T_{ph}^6), \quad (2)$$

where  $\Sigma = 2.3 \cdot 10^9 \text{ W/m}^3 \text{ K}^6$ . Similar dependencies were measured in thin aluminum films doped with manganese [6] and in Hf and Ti films [7].

In addition to these dependences, in the literature, one can find other models of electron-phonon relaxation, and power-law dependences from  $T^4$  to  $T^6$ , related to the so-called dirty limit with a short electron mean free path. In the case of detachment of the absorber from the substrate, when electrons are considered in a three-dimensional model and absorber phonons in a two-dimensional model, the exponent is 4.54 in 2D limit and  $n = 6 \dots 7$  in bulk limit [8], [9]. In the general case, the thermal conductivity between electrons and phonons is inversely proportional to the electron-phonon relaxation time  $G_{ep} = C/\tau_{ep}$ , where the electronic heat capacity is  $C = \gamma v T$  and  $\gamma$  is the Sommerfeld constant. If the relaxation time depends on temperature as  $\tau_{ep}^{-1} = \alpha T^m$  and the thermal conductivity is proportional to  $G_{ep} = \alpha \gamma v T^{m+1}$ , then the power of the electron-phonon heat exchange  $P_{e-ph} = (\alpha v \gamma / (m+2)) (T^{m+2} - T_{ph}^{m+2})$ . The exponent in different publications is  $m = 2$ ,  $m = 3$ , or  $m = 4$ . In theory, for pure bulk metals and three-dimensional phonons,  $m = 3$ . However, in thin films in the dirty limit, the Echternach theory [10] predicts  $m = 4$ . Formula (2) should be used for three-dimensional phonons, and for two-dimensional phonons again  $m = 3$ , i.e., formula (1). According to [11], for thin films with an electron mean free path of less than 3 nm, the dependence of the relaxation time corresponds to  $m = 4$  at  $T < 3 \text{ K}$  and  $m = 2$  at  $T > 20 \text{ K}$ . It means that for the power of the electron-phonon interaction, the dependence varies from  $T^6$  to  $T^4$ . Which ratio should be used in specific cases depends on the thickness, composition, and quality of the films and requires experimental verification to correctly estimate the power and temperature.

## II. EXPERIMENTAL

We studied the receiver in the form of a matrix of  $5 \times 5$  ring planar antennas. The rings were cut in halves and SINIS structures were inserted into the gaps, where S is aluminum

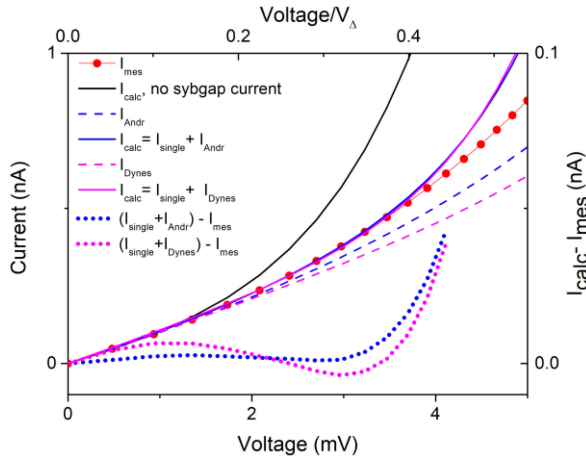


Fig. 1. Measured IV curves of SINIS at 0.1 K (dots) and simulation of equivalent  $T_e$  with (blue or magenta) and without (black) lines accounting for subgap Andreev or Dynes current for the same  $R_d$  at zero bias and  $\gamma=10^{-7}\Omega^{-1}$ .

superconducting electrodes, I is an aluminum oxide tunnel barrier, N is a layer of non-superconducting aluminum with thin iron sublayer [12], [13]. For direct current bias, the rings are connected in series. Thus, 25 serially connected SINIS form 2 parallel connected chains. Matrix dimensions are 2.2 by 2.2 mm<sup>2</sup>. The area of the normal electrode of each NIS in thermal contact with the silicon substrate is 0.8  $\mu\text{m}^2$ , thickness is 0.02  $\mu\text{m}$ . Thus, the total area of all normal electrodes is 80  $\mu\text{m}^2$ , their volume is 1.6  $\mu\text{m}^3$ .

The experiments were carried out using a miniature dilution cryostat [14] at temperatures in the range 0.1–0.3 K. The receiver was irradiated with a black body radiation source - a NiCr film on a silicon substrate, heated when the voltage  $U_{\text{rad}}$  was applied in the range 0–10 V within the temperature range 0.7–15 K. The radiation passed through a narrow-band interference filter with a central frequency of 330 GHz and focused on the receiving structure by a sapphire immersion lens. An example of the I-V characteristic measured at 0.1 K is shown in Fig. 1. To calculate  $T_e$ , we use a simplified formula for the single-electron current of an ideal NIS junction [15]

$$I(V, T_e) = \left( \frac{1}{eR_n} \right) \sqrt{2\pi kT_e E_\Delta} \exp\left(\frac{-E_\Delta}{kT_e}\right) \sinh\left(\frac{eV}{kT_e}\right). \quad (3)$$

Here  $R_n$  is the normal resistance of single junction at  $T > T_c$ ,  $E_\Delta$  is the superconducting gap energy,  $k$  is the Boltzmann constant, and  $e$  is the electron charge. Its accuracy is sufficient when the voltage across the structure is  $V < V_\Delta = NE_\Delta/e$  and  $T < < T_c$ . For temperatures in 0.1–0.3 K range the difference between  $T_e$ , calculated by exact integral equation and approximate equation (3), is 1–2 mK and doesn't exceed the measurement accuracy.

If we assume that the I-V characteristic in Fig. 1 corresponds to a single-electron current according to formula (3), then at  $V = 0$  the electron temperature exceeds 0.3 K, which could be explained by strong overheating of the receiver by parasitic radiation. To create such overheating, power of the order of

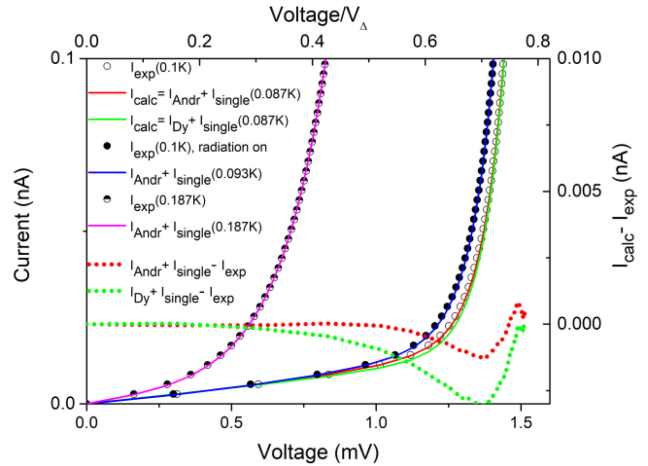


Fig. 2. Measured (symbols) and calculated (lines) IV curves for NIS thermometer array at bath temperatures 0.1 and 0.187 K.

5–10 pW must be absorbed, which is not the case. However, the  $T_e$  estimate by formula (3) already at  $V/V_\Delta \sim 0.1$  noticeably decreases, although electron cooling, whose power is an order of magnitude less than  $VI$  and does not exceed 0.05 pW, is clearly insufficient for this case. Therefore, the single-electron current of the ideal NIS junction according to formula (3) at low voltages is only a small fraction of the total current, the contribution to which can due to the subgap Andreev current  $I_n + I_s$  [13], [16]. In the case of electrons scattering by magnetic ions, as established in [16], [17],  $I_n$  is near zero and  $I_s$  can be presented as

$$I_s = \frac{\gamma V}{\sqrt{1 - V/V_\Delta}}. \quad (4)$$

This formula valid for  $(\hbar D/E_\Delta)^{1/2} \ll L$ , where  $L \sim 1\mu\text{m}$  is the lateral size of the junction,  $D$  - diffusion coefficient. For Al films  $D \sim 50\text{ cm}^2/\text{s}$  [17].

As well as Dynes current  $I_{\text{Dy}}$  [5], that is usually attributed to smearing of the superconductor energy gap:

$$I_{\text{Dy}} = \frac{\gamma V}{\sqrt{1 - (V/V_\Delta)^2}}. \quad (5)$$

In these formulas,  $\gamma$  is the coefficient chosen for better matching of the I-V characteristic with the calculated current, while selecting  $T_e$  in formula (3) [19], [20]. At  $V/V_\Delta < 0.3$  obtained  $T_e$  values slightly differ, which does not affect the results. But at low voltages there is a qualitative difference - the differential conductivity according to formula (4) changes linearly, which corresponds to experiment [17], [18]. Equation (5) is similar to the calculation of Andreev current in [19]. Similar features were observed in [20]. But in our case equation (5) deviates from our experimental data, presented on Figs. 1 and 2. Based on this, further in the calculations we used only formula (4).

Good agreement between the experimental and calculated IV characteristics, Fig. 1, is achieved at  $V/V_\Delta < 0.3$  at  $T_e = 0.21\text{ K}$ , which is much higher than the substrate temperature. This indicates that parasitic radiation hits the receiver and, as a consequence, overheating of electrons relative to the substrate

TABLE I  
THE VALUES OF THE ELECTRON-PHONON INTERACTION POWER AT T = 0.1 K  
FOR VARIOUS RADIATION POWER LEVELS CORRESPONDING TO THE U<sub>RAD</sub>  
VOLTAGE APPLIED TO THE RADIATION SOURCE

U <sub>rad</sub> , V	0	4	6	8
P <sub>e-ph</sub> = vΣ(T <sub>e</sub> <sup>5</sup> - T <sub>ph</sub> <sup>5</sup> ), pW	0.8	3.9	8.3	14.0
P <sub>e-ph</sub> = vΣ(T <sub>e</sub> <sup>6</sup> - T <sub>ph</sub> <sup>6</sup> ), pW	0.3	1.9	4.7	8.8

and also indicates the presence of thermal resistance between the electron system and the substrate. The influence of thermal resistance between substrate and the thermostat is negligible and estimated by means of NIS thermometer placed on the substrate in addition to the receiving structure.

The NIS thermometer consists of 10 identical cells connected in series. Each cell contains a wiring conductor made of gold and palladium bilayer film, on which a layer of aluminum is deposited, on the other side covering a normal layer of aluminum with an iron sublayer through the aluminum oxide layer. Tunnel junction area is 2  $\mu\text{m}^2$ . The normal layer following the tunnel contact, lies directly on the next AuPd wiring line. Thus, the total volume of normal metal in each cell is large enough to ensure efficient thermalization of electrons. This conclusion is confirmed by the measurement results in Fig. 2. At voltages  $V/V_\Delta < 0.5$ , the current is completely due to the Andreev contribution, formula (4) is valid, and only at high voltages there is the visible contribution of the single-electron current corresponding to  $T_e = 0.087$  K, which is even slightly lower than the readings of a ruthenium oxide thermometer mounted on the sample holder. For such thermometers, the effect of stray illumination on their resistance is well known. But in the future, when determining the power of the electron-phonon interaction, we will rely on the readings of a ruthenium thermometer, which continuously monitors the temperature, since this leads to an error of e-ph power less than 2% at the lowest temperature [see Table I].

Under irradiation of a sample with a receiving structure that absorbs a power of about 5 pW, at which its electron temperature  $T_e$  increases from 0.21 to ~0.3 K, the temperature of the NIS thermometer changes by only 5 mK. The rise time of the thermometer response is of the order of a minute when the radiation source is turned on, while the temperature of source rises twice as fast. This result reflects the heating of the entire substrate. For comparison, the response time constant of the receiving structure is 20  $\mu\text{s}$  [21]. The gradient estimate is less than 0.1 mK/mm. So, the heating of the substrate can be neglected.

When analyzing the experiments, it was assumed that the power absorbed by the SINIS does not depend on temperature, since the signal from the antennas is transmitted to the absorber — a normal electrode, whose resistance does not depend on temperature, through the capacitance of tunnel junctions. Its impedance at high frequencies of the order of 0.01–0.1  $\Omega$  is much less compared to the resistance of the absorber. At temperatures of ~0.1 K and 0.3 K,  $T_e$  values were calculated taking into account the Andreev current (4), which does not depend on temperature. The values of  $T_e(U_{rad} = 0)$  were determined at a certain starting value of  $E_\Delta$ . Using formulas (1) or (2) at

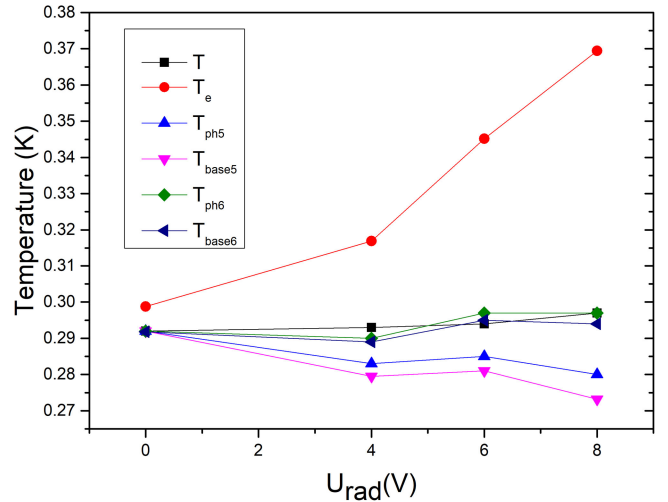


Fig. 3. The bath temperature T, the electron temperature T<sub>e</sub>, calculated phonon temperatures T<sub>ph5</sub>, T<sub>ph6</sub> and considering Kapitza resistance substrate temperatures T<sub>base5</sub>, T<sub>base6</sub>. The values of the electron-phonon interaction power at T = 0.1 K were used for calculations are given in Table I.

$T_{ph} = T \sim 0.1$  K, the values of  $P_5(U_{rad} = 0)$  and  $P_6(U_{rad} = 0)$ , due to the absorption of parasitic radiation, were calculated. Then the values of  $T_{ph}(U_{rad})$  were refined and an amendment was made to  $P_5$ ,  $P_6$ , taking into account the Kapitza resistance and the continuity of the energy flow [3]:

$$P_K = \xi s (T_{ph}^4 - T^4), \quad (6)$$

where  $\xi = 360 \text{ nW}/\mu\text{m}^2\text{K}^4$ , s is the contact area of the normal electrode with the substrate. This correction in all cases did not exceed 1-2%.

Temperature of bath T, electron temperature T<sub>e</sub>, and recalculated phonon temperatures T<sub>ph5</sub> and T<sub>ph6</sub> at which electron-phonon power provide it at T = 0.1 K for different radiation power levels determined by voltage U<sub>rad</sub> applied to radiation source.

At the next step, the values of equivalent phonon temperatures T<sub>ph5</sub>(U<sub>rad</sub> = 0), (or T<sub>ph6</sub>(U<sub>rad</sub> = 0)) were calculated from (1) and (2) using the values of T<sub>e</sub> set at the temperature  $T \approx 0.3$  K and the power P<sub>5</sub>(U<sub>rad</sub> = 0) (or P<sub>6</sub>(U<sub>rad</sub> = 0)). Finally, we calculated the equivalent phonon temperatures T<sub>base5</sub> (or T<sub>base6</sub>), that in addition are taking into account the correction for the Kapitza resistance corresponding to power flow. If T<sub>ph5</sub>(U<sub>rad</sub> = 0), respectively T<sub>ph6</sub>(U<sub>rad</sub> = 0), did not coincide with the temperature T, when the radiation effect was minimal, the values of E<sub>Δ</sub> were refined. They become equal to E<sub>Δ</sub> = 2.20 kJ and 2.17 kJ for models (1) and (2), respectively. Thus, E<sub>Δ</sub> turns to be the model dependent parameter because of the insufficient precision in V<sub>Δ</sub> which is given by the peak of the conductance at low temperatures.

As can be seen from Fig. 3, under this condition T<sub>base6</sub> = T with an accuracy of  $\pm 4$  mK, which corresponds to the error in determining T<sub>e</sub> of  $\pm 1$  mK, in the range U<sub>rad</sub> = 0 – 8 V, while power P<sub>e-ph</sub> varies within 0.4–9 pW, and T<sub>e</sub> increases from 0.3 to 0.38 K. In contrast, T<sub>base5</sub> with an increase in the radiation power becomes less than T<sub>base</sub> on average by ~10 mK. Thus,

preference should be given to formula (2) when describing the electron - phonon interaction for aluminum on silicon. Note that these results do not depend on the specific values of the coupling constants. They practically do not depend on the choice of the coefficient in the formula for the subgap current. If we assume that it does not exist at all, then qualitatively the result differs little from that presented in Fig. 3.

Let us give typical examples of the difference in the results of estimates for these models for the case of  $T_{ph} = 0.1$  K,  $T_e = 0.3$  K,  $v = 1 \mu\text{m}^3$ , we obtain by formula (1)  $P_5 = 3.1$  pW and by formula (2)  $P_6 = 1.6$  pW, i.e., the difference is almost twofold. It is also useful to compare the estimates of the electron temperature for these two cases. If the electron temperature noticeably exceeds the phonon temperature, then for an absorbed power of 0.1 pW, the electron temperature estimate will be  $T_{e5} = 0.15$  K and  $T_{e6} = 0.187$  K, i.e., the difference is almost 40 mK. The use of the model with the fifth power gives too optimistic underestimated values of the electron temperature.

## REFERENCES

- [1] M. Nahum and J. M. Martinis, "Ultrasensitive-hot-electron microbolometer," *Appl. Phys. Lett.*, vol. 63, 1993, Art. no. 3075, doi: [10.1063/1.110237](https://doi.org/10.1063/1.110237).
- [2] L. S. Kuzmin *et al.*, "Photon-noise-limited cold-electron bolometer based on strong electron self-cooling for high-performance cosmology missions," *Commun. Phys.*, vol. 2, 2019, Art. no. 104, doi: [10.1038/s42005-019-0206-9](https://doi.org/10.1038/s42005-019-0206-9).
- [3] V. F. Gantmakher, "The experimental study of electron-phonon scattering in metals," *Rep. Prog. Phys.*, vol. 37, no. 3, 1974, Art. no. 317, doi: [10.1088/0034-4885/37/3/001](https://doi.org/10.1088/0034-4885/37/3/001).
- [4] A. Gunbina, S. A. Lemzyakov, M. A. Tarasov, V. S. Edelman, and R. A. Yusupov, "Response of a SINIS detector with electron cooling to submillimeter-wave radiation," *JETP Lett.*, vol. 111, no. 10, pp. 539–542, 2020, doi: [10.1134/S0021364020100094](https://doi.org/10.1134/S0021364020100094).
- [5] G. C. O'Neil, P. J. Lowell, J. M. Underwood, and J. N. Ullom, "Measurement and modeling of a large-area normal-metal/insulator/superconductor refrigerator with improved cooling," *Phys. Rev.*, vol. 85, 2012, Art. no. 134504, doi: [10.1103/PhysRevB.85.134504](https://doi.org/10.1103/PhysRevB.85.134504).
- [6] L. J. Taskinen and I. J. Maasilta, "Improving the performance of hot-electron bolometers and solid state coolers with disordered alloys," *Appl. Phys. Lett.*, vol. 89, 2006, Art. no. 143511, doi: [10.1063/1.2357555](https://doi.org/10.1063/1.2357555).
- [7] M. E. Gershenson, D. Gong, and T. Sato, "Millisecond electron-phonon relaxation in ultrathin disordered metal films at millikelvin temperatures," *Appl. Phys. Lett.*, vol. 79, no. 13, 2001, Art. no. 2049, doi: [10.1063/1.1407302](https://doi.org/10.1063/1.1407302).
- [8] J. T. Karvonen and I. J. Maasilta, "Influence of phonon dimensionality on electron energy relaxation," *Phys. Rev. Lett.*, vol. 99, 2007, Art. no. 145503, doi: [10.1103/PhysRevLett.99.145503](https://doi.org/10.1103/PhysRevLett.99.145503).
- [9] O.-P. Saira, M. H. Matheny, L. Wang, J. Pekola, and M. Roukes, "Modification of electron-phonon coupling by micromachining and suspension," *J. Appl. Phys.*, vol. 127, 2020, Art. no. 024307, doi: [10.1063/1.5132948](https://doi.org/10.1063/1.5132948).
- [10] P. M. Echternach, M. R. Thoman, C. M. Gould, and H. M. Bozler, "Electron-phonon scattering rates in disordered metallic films below 1 K," *Phys. Rev.*, vol. 46, no. 16, pp. 10339–10334, 1992, doi: [10.1103/PhysRevB.46.10339](https://doi.org/10.1103/PhysRevB.46.10339).
- [11] A. Sergeev and V. Mitin, "Electron-phonon interaction in disordered conductors: Static and vibrating scattering potentials," *Phys. Rev.*, vol. 61, no. 9, pp. 6041–6047, 2000, doi: [10.1103/PhysRevB.61.6041](https://doi.org/10.1103/PhysRevB.61.6041).
- [12] M. A. Tarasov *et al.*, "Arrays of annular antennas with SINIS bolometers," *IEEE Trans. Appl. Supercond.*, vol. 30, no. 3, Apr. 2020, Art. no. 2300106, doi: [10.1109/TASC.2019.2941857](https://doi.org/10.1109/TASC.2019.2941857).
- [13] M. A. Tarasov, A. M. Chekushkin, R. A. Yusupov, A. A. Gunbina, and V. S. Edelman, "Matching of radiation with array of planar antennas with SINIS bolometers in an integrating cavity," *J. Commun. Technol. Electron.*, vol. 65, no. 1, pp. 60–68, 2020, doi: [10.1134/S1064226920010064](https://doi.org/10.1134/S1064226920010064).
- [14] V. S. Edelman, "A dilution microcryostat-insert," *Instruments Exp. Techn.*, vol. 52, no. 2, pp. 301–307, 2009, doi: [10.1134/S002044120902033X](https://doi.org/10.1134/S002044120902033X).
- [15] M. Nahum, P. L. Richards, and C. A. Mears, "Design analysis of a novel hot-electron microbolometer," *IEEE Trans. Appl. Supercond.*, vol. 3, no. 1, pp. 2124–2127, Mar. 1993, doi: [10.1109/77.233921](https://doi.org/10.1109/77.233921).
- [16] F. W. J. Hekking and Y. V. Nazarov, "Subgap conductivity of a superconductor-normal-metal tunnel interface," *Phys. Rev.*, vol. 49, 1994, Art. no. 6847, doi: [10.1103/PhysRevB.49.6847](https://doi.org/10.1103/PhysRevB.49.6847).
- [17] A. V. Seliverstov, M. A. Tarasov, and V. S. Edelman, "The Andreev conductance in superconductor-insulator-normal metal structures," *J. Exp. Theor. Phys.*, vol. 124, no. 4, pp. 643–656, 2017, doi: [10.1134/S1063776117030153](https://doi.org/10.1134/S1063776117030153).
- [18] M. Tarasov *et al.*, "Fabrication of NIS and SIS nanojunctions with aluminum electrodes and studies of magnetic field influence on IV curves," *Electronics*, vol. 10, no. 23, 2021, Art. no. 2894, doi: [10.3390/electronics10232894](https://doi.org/10.3390/electronics10232894).
- [19] T. Faivre, D. S. Golubev, and J. P. Pekola, "Andreev current for low temperature thermometry," *Appl. Phys. Lett.*, vol. 106, 2015, Art. no. 182602, doi: [10.1063/1.4919892](https://doi.org/10.1063/1.4919892).
- [20] T. Greibe, M. Stenberg, C. Wilson, T. Bauch, V. Shumeiko, and P. Delsing, "Are pinholes the cause of excess current in superconducting tunnel junctions? A study of andreev current in highly resistive junctions," *Phys. Rev. Lett.*, vol. 106, 2011, Art. no. 097001, doi: [10.1103/PhysRevLett.106.097001](https://doi.org/10.1103/PhysRevLett.106.097001).
- [21] S. Lemzyakov, M. Tarasov, S. Mahashabde, R. Yusupov, L. Kuzmin, and V. Edelman, "Experimental study of a SINIS detector response time at 350 GHz signal frequency," *J. Phys.: Conf. Ser.*, vol. 969, 2018, Art. no. 012081, doi: [10.1088/1742-6596/969/1/012081](https://doi.org/10.1088/1742-6596/969/1/012081).